Tunable double-resonance dimer structure for surface-enhanced Raman scattering substrate in near-infrared region

Zhengqing Qi,[1] Jie Yao,[1,2] Liangliang Zhao,[1] Yiping Cui,[1] and Changgui Lu[1,*]

[1]*Advanced Photonics Center, Southeast University, Nanjing 210096, China*
[2]*Nanjing Normal University, Nanjing 210023, China*
**Corresponding author: changguilu@seu.edu.cn*

Received May 28, 2015; revised August 22, 2015; accepted August 25, 2015;
posted September 10, 2015 (Doc. ID 241870); published October 19, 2015

Plasmonic resonance with Fano lineshape has attracted a great deal of recent interest. Here we design a new structure with a dimer grating upon a gold film separated by a layer of silica spacer, which has two resonant modes corresponding to the dimer's localized surface plasmon resonance and the surface plasmon resonance excited by the dimer grating. This structure has three advantages for near-infrared detection in water. First, it provides two resonant modes to enhance the excitation and scattered signals of surface-enhanced Raman scattering. Second, coupling of these two modes results in a Fano resonance, providing a higher electric field enhancement. Finally, the dimer provides more flexible tunability compared to a single disk structure.

OCIS codes: (250.5403) Plasmonics; (240.6695) Surface-enhanced Raman scattering.
http://dx.doi.org/10.1364/PRJ.3.000313

1. INTRODUCTION

Surface-enhanced Raman scattering (SERS) is an important application of surface plasmon polaritons (SPPs) and has great potential for biological sensing [1,2]. Recently, increasing interest has been focused on the near-infrared (NIR) region, where blood and tissue are mostly transparent and light can penetrate tissues deeply, giving a chance for SERS to be utilized *in vivo* [3,4]. Due to the effect of "hot spots," structures composed of nanoscale noble metal particles provide strong Raman signals when molecules are absorbed at or near the surface of nanoparticles. Structures composed of unordered metallic nanoparticles [5–7] have been studied and provide high SERS enhancement factors up to 10^{14}. With the development of micro–nano processing technology, metallic nanostructures such as nanodisks [8], nanorings [9], and nanorods [10] are proposed to achieve more stable and reproducible SERS substrates. Recent studies have proved that it is an effective way to achieve a high local electric field and tune the plasmon resonances by putting metallic nanostructures on metal films [11,12]. For example, Kim and Cheng found high optical field enhancements at the edges of the nanostructures originating from coupling of localized surface plasmon resonance (LSPR) and gap SPPs. They predicted such SERS enhancement factors of up to 10^{11} for equilateral triangular nanostructures [11]. Lévêque and Martin have reported that setting gold nanosquares on a gold film can modify the plasmon resonance wavelength from 600 to 900 nm by changing the dielectric spacer thickness [12].

It is well accepted that the SERS enhancement is proportional to the product of the local electric intensities both at the frequency of exciting light and at the Stokes frequency of scattered light [13]. Based on this theory, periodic nanostructures upon metallic film separated by a dielectric layer are introduced to provide double-resonance substrates for selective Raman signal enhancements [14,15]. For such structures, SPPs supported by the grating strongly couple with the localized surface plasmons of gold nanodisks, resulting in double resonances.

In this paper, we convert the single disk array into a pair disk array [16] and change the surrounding material from air to water, which provides a promising substrate for SERS detection in biological media. According to the analysis of Hao and Schatz [7], the SERS enhancement factors in dimer structures are a factor of 10 larger than those in monomers. Besides, the water environment also provides a minor refractive index contrast between water and glass substrates compared with the air environment, which enables lager field enhancements. We optimize the coupling efficiency between surface plasmon resonance (SPR) and LSPR by tuning the thickness of the dielectric spacer. By tuning the interval of the gold nanoparticle pair, we realize the modulation of the LSPR wavelength and provide higher electric field intensity than that in the single disk case.

2. SIMULATION MODELS

The structure under investigation includes an array of gold disk pairs upon gold film separated by a silica spacer. The schematic of the structure is shown in Fig. 1. The finite-element method is used to calculate the near field of the structure. The normally incident light is polarized along the x direction. The diameter and the thickness of the disk are set as 130 and 30 nm to get a LSPR mode in the NIR region that can couple with the SPR mode excited by the dimer grating. The thickness of the gold film is 150 nm, large enough to prevent LSPR

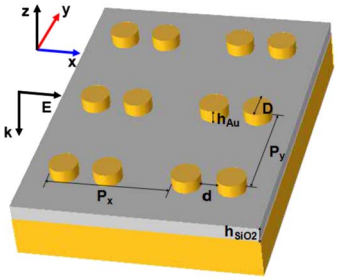

Fig. 1. Schematic of double-resonance gold dimer array substrate.

coupling with the bottom side of the film. The dielectric permittivity of gold is taken from Johnson and Christy's experimental data [17]. The refractive index of silica is set to a constant value of 1.45 with the neglect of frequency change [18]. The near field of the gold nanoparticle pairs is calculated for different structure parameters.

The enhancement factor of SERS [19,20] can be expressed as

$$G_{\mathrm{SERS}} \propto \left|\frac{E_{\mathrm{loc}(\lambda_{\mathrm{exc}})}}{E_{\mathrm{inc}(\lambda_{\mathrm{exc}})}}\right|^2 \left|\frac{E_{\mathrm{loc}(\lambda_{\mathrm{Raman}})}}{E_{\mathrm{inc}(\lambda_{\mathrm{Raman}})}}\right|^2, \tag{1}$$

where $E_{\mathrm{loc(exc)}}$ and $E_{\mathrm{inc(exc)}}$ are the local electric field and incident electric field of the exciting wavelength, respectively. $E_{\mathrm{loc(Raman)}}$ and $E_{\mathrm{inc(Raman)}}$ represent the local and the incident electric fields at the Raman scattered wavelength. According to this equation, we take a product of the near-field intensity enhancements at LSPR and SPR wavelengths to qualitatively estimate the G_{SERS}.

To excite the SPR mode of the gold film, an external wavevector should be supplied by the grating [21], which can be expressed as

$$k_{\mathrm{spp}} = k_{\parallel} \pm \frac{G}{n}\sqrt{i^2 + j^2}, \tag{2}$$

where $G = 2\pi/P_x$ is the reciprocal grating vector of the structure with x-direction grating constant P_x, (i, j) denotes the grating diffraction order, $k_{\parallel}$ is the wavevector component of incident light along the surface, and n is the refractive index of water. Under normal incidence we have $k_{\parallel} = 0$; the first-order SPP mode occurs when the wavevector satisfies the equation $k_{\mathrm{spp}} = G/n$. Here we fix the period of the x direction as 550 nm, which makes the wavelength of the SPP mode almost constant by ignoring slight wavelength variations caused by other geometrical parameter changes. This special characteristic provides a reasonable usage at the excited wavelength of SERS. Besides, the sharper Q factor of the SPP and the broader Q factor of LSPR also exhibit a rational property in the application of the SERS substrate.

3. SIMULATION RESULTS AND DISCUSSION

Before optimizing the dimer grating structure, we simulate four structures, as shown in Fig. 2(c), to compare the electric intensity enhancement factors. The grating constants P_x and P_y are set to 550 and 500 nm, respectively. The gold nanodisk is 30 nm high and 130 nm in diameter, and the interval of the dimer is 15 nm.

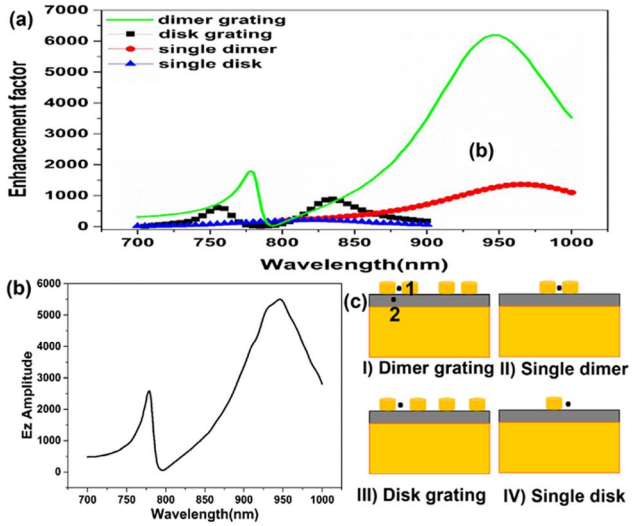

Fig. 2. (a) Simulated electric field intensity enhancement factors of the dimer grating (green solid line), the single disk grating (black square line), a single dimer (red circle line), and a single disk (blue triangle line) upon gold film separated by a layer of silica spacer. (b) Ez amplitude at position 2 for the gold dimer array case. (c) Schematics of the four structures simulated.

As shown in Fig. 2(a), the structures with the dimer grating and the single disk grating exhibit two resonant modes, corresponding to the LSPR mode and the SPR mode, respectively. Besides, the electric field intensity in the dimer grating is larger than that in the other three structures, which is caused by the interaction of the disks of the dimer and the Fano resonance resulting from the coupling between the SPR mode and the LSPR mode. The amplitude of Ez of the SPR on the gold film at position 2 is shown in Fig. 2(b), which behaves similarly with the near-field enhancement factor.

The two resonant modes in the dimer array case, respectively, correspond to the SPR [Fig. 3(a)] and LSPR [Fig. 3(b)] as the thickness of the silica spacer is 45 nm and the separation of the dimer is 15 nm. Figure 3(a) exhibits an obvious grating-like electric field distribution, while Fig. 3(b) shows that the electric field is mainly confined in the gap of the disk pair. As we know, the SPR mode is mainly determined by the array period and exhibits a global electric field distribution with interference strikes on the surface of

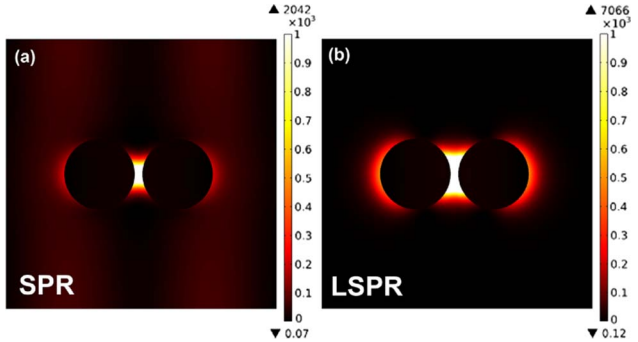

Fig. 3. (a) Intensity ($|E|^2$) distribution on the half-height surface of the gold disk with $h_{SiO_2} = 45$ nm at 785 nm (SPR) with maximum intensity 2042. (b) 950 nm (LSPR) with maximum intensity 7066 corresponding to the two resonant modes of the dimer grating case in Fig. 2(a), respectively.

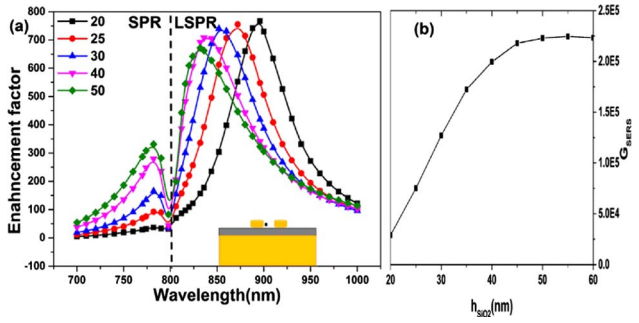

Fig. 4. (a) Simulated electric field spectrum for the structure with $P_x = 550$ nm, $P_y = 500$ nm, and $d = 60$ nm at different thicknesses of the silica spacer. (b) Holistic enhancement G_{SERS} via the change of the thickness of the silica spacer.

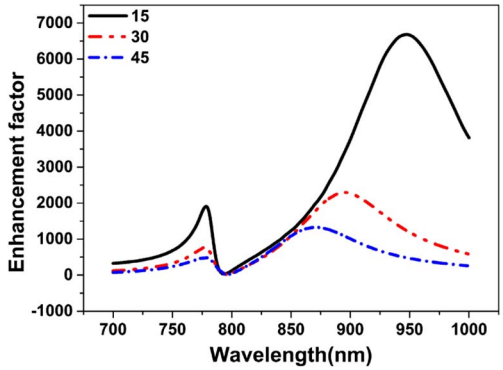

Fig. 5. Electric field spectrum with $P_x = 550$ nm, $P_y = 500$ nm, and $h_{\mathrm{SiO_2}} = 45$ nm at different interparticle separations: 15 nm (black line), 30 nm (red dot-dotted dash line), and 45 nm (blue dotted–dashed line).

the whole structure. The LSPR mode of the dimer has the feature of high field enhancement, which is mainly localized between the disks. So the electric field distribution shown in Fig. 3(a) is related to the SPR mode, and that in Fig. 3(b) corresponds to the LSPR mode. Besides, the highly confined electric field in the gap means that this structure possesses good spatial selection.

Figure 4(a) shows the influence of the silica spacer thickness. Keeping the other parameters unchanged when the silica spacer thickness increases, the LSPR presents an obvious blue shift due to the weaker coupling between the gold nanoparticle pairs and its image in the gold film. A slight wavelength change of the SPR mode is observed due to the increase of the effective refractive index above the gold film.

In order to obtain an optimal thickness of the silica spacer, we investigate how G_{SERS} changes with the thickness of the dielectric layer based on Eq. (1). An asymptotically stable enhancement via the increase of the silica spacer thickness is obtained, as shown in Fig. 3(b), which helps us to determine 45 nm as the optimal thickness of the silica spacer.

To study the LSP resonance quality of this double-resonant substrate, the effective mode volume normalized to $(\lambda/2)^3$, V_{eff}, the quality factor Q, and the ratio of these two values Q/V_{eff} are calculated, as shown in Table 1. The effective mode volume V_{eff} is calculated based on theories discussed in Refs. [22,23]. The quality factor Q is calculated by fitting the simulated spectral to Lorentzian functions to estimate the full width half-maximum of the resonance [24]. As the interparticle distance increases, both the V_{eff} and the Q factor become larger for the weaker interaction between the disks of the dimer. Besides, we also calculate these parameters with a single dimer with the gap of 15 nm and a single disk separated from gold film by a 45 nm thick layer of silica spacer, which are listed in the last two rows of Table 1. We find that the gold dimer grating structures have a larger Q/V_{eff} compared to the single dimer and the single disk with the gold film and silica spacer unchanged, which represents a higher enhancement gain in SERS. Therefore, the structure with the gold dimer array is more suitable for the SERS substrate than that without an array.

Table 1. Normalized Effective Mode Volume and the Quality Factor for Different Interparticle Separation Dimers, a Single Dimer with a Gap of 15 nm, and a Single Disk upon Gold Film Separated by a Layer of Silica Spacer

d (nm)	V_{eff}	Q	Q/V_{eff}
15	1.16E – 4	8.48	7.33E4
20	1.59E – 4	9.07	5.69E4
25	2.05E – 4	9.68	4.71E4
30	2.45E – 4	10.16	4.14E4
35	2.84E – 4	10.55	3.71E4
45	3.61E – 4	11.45	3.17E4
65	4.78E – 4	13.34	2.79E4
Single dimer with a gap of 15 nm	2.71E – 4	4.04	1.49E4
Single disk	1.33E – 3	5.96	4.48E3

To modulate the LSPR mode, methods by changing the grating constant, the diameter and thickness of the disks, and the thickness of the spacer have been proposed and analyzed in the last few years. Here, we provide an additional method to modulate the LSPR mode by varying the gap of the dimer. Figure 5 presents the simulated electric field intensity enhancement factor around the Au-nanodisk-pairs–silica–Au-film structures with the gap changed from 15 to 45 nm. The grating constant, the silica spacer, and the parameters of the disk are unchanged. As the gap increases, the LSPR mode shows a significant blue shift as the interaction of the disks becomes weaker, while the SPR mode corresponding to the incident frequency is almost unchanged. The LSPR's blue shift with the increase of the interparticle separation was demonstrated experimentally by Jain *et al.* [25,26]. When two disks are close to each other, they form dipole–dipole coupling. The LSPR mode of the dimer corresponds to the bonding mode [27]. With the increase of the separation distance in dimers, the coupling of the two particles becomes weaker and the LSPR mode moves toward the dipole mode of individual disks. This property provides an additional method for the wavelength modulation along different electric field enhancements for SERS detection.

4. CONCLUSIONS

In conclusion, we propose a SERS substrate with extremely high field enhancements between the dimer at both excitation and Stokes frequencies. Compared to the single disk structure, the dimer grating structure possesses not only higher excitation efficiency of SPPs at the shorter wavelength resonance, but also a higher Q factor and a relatively smaller mode volume resulting from the dimer gap. Furthermore, the SPR

and the LSPR form a Fano resonance that provides higher SERS enhancement. Such a dimer structure can also be designed to have three or even more resonant modes by introducing multilayers into disks, which can specifically enhance more Stokes frequencies of target molecules besides the excitation frequency to improve recognition.

ACKNOWLEDGMENT

This work is supported by the National Science Foundations of China (Grant No. 11274062) and the Program of Natural Science Research of Jiangsu Higher Education Institutions of China (Grant No. 14KJB510016).

REFERENCES

1. A. Gopinath, S. V. Boriskina, W. R. Premasiri, L. Ziegler, B. M. Reinhard, and L. D. Negro, "Plasmonic nanogalaxies: multiscale aperiodic arrays for surface-enhanced Raman sensing," Nano Lett. **9**, 3922–3929 (2009).
2. D. Wang, W. Zhu, Y. Chu, and K. B. Crozier, "High directivity optical antenna substrates for surface enhanced Raman scattering," Adv. Mater. **24**, 4376–4380 (2012).
3. M. Shioi, H. Jans, K. Lodewijks, P. Van Dorpe, L. Lagae, and T. Kawamura, "Tuning the interaction between propagating and localized surface plasmons for surface enhanced Raman scattering in water for biomedical and environmental applications," Appl. Phys. Lett. **104**, 243102 (2014).
4. J. Ye, M. Shioi, K. Lodewijks, L. Lagae, T. Kawamura, and P. Van Dorpe, "Tuning plasmonic interaction between gold nanorings and a gold film for surface enhanced Raman scattering," Appl. Phys. Lett. **97**, 163106 (2010).
5. J. F. Li, Y. F. Huang, Y. Ding, Z. L. Yang, S. B. Li, X. S. Zhou, F. R. Fan, W. Zhang, Z. Y. Zhou, D. Y. Wu, B. Ren, Z. L. Wang, and Z. Q. Tian, "Shell-isolated nanoparticle-enhanced Raman spectroscopy," Nature **464**, 392–395 (2010).
6. C. E. Talley, J. B. Jackson, C. Oubre, N. K. Grady, C. W. Hollars, S. M. Lane, T. R. Huser, P. Nordlander, and N. J. Halas, "Surface-enhanced Raman scattering from individual Au nanoparticles and nanoparticle dimer substrates," Nano Lett. **5**, 1569–1574 (2005).
7. E. Hao and G. C. Schatz, "Electromagnetic fields around silver nanoparticles and dimmers," J. Chem. Phys. **120**, 357–366 (2004).
8. J. Qi, P. Motwani, M. Gheewala, C. Brennan, J. C. Wolfe, and W. C. Shih, "Surface-enhanced Raman spectroscopy with monolithic nanoporous gold disk substrates," Nanoscale **5**, 4105–4109 (2013).
9. J. Aizpurua, P. Hanarp, D. S. Sutherland, M. Kall, G. W. Bryant, and F. J. G. de Abajo, "Optical properties of gold nanorings," Phys. Rev. Lett. **90**, 057401 (2003).
10. J. Aizpurua, G. W. Bryant, L. J. Richter, F. J. G. de Abajo, B. K. Kelley, and T. Mallouk, "Optical properties of coupled metallic nanorods for field-enhanced spectroscopy," Phys. Rev. B **71**, 235420 (2005).
11. H. C. Kim and X. Cheng, "SERS-active substrate based on gap surface plasmon polaritons," Opt. Express **17**, 17234–17241 (2009).
12. G. Lévêque and O. J. F. Martin, "Tunable composite nanoparticle for plasmonics," Opt. Lett. **31**, 2750–2752 (2006).
13. Y. Chu, M. G. Banaee, and K. B. Crozier, "Double-resonance plasmon substrates for surface-enhanced Raman scattering with enhancement at excitation and Stokes frequencies," ACS Nano **4**, 2804–2810 (2010).
14. Y. Chu, D. Wang, W. Zhu, and K. B. Crozier, "Double resonance surface enhanced Raman scattering substrates: an intuitive coupled oscillator model," Opt. Express **19**, 14919–14928 (2011).
15. Y. Chu, E. Schonbrun, T. Yang, and K. B. Crozier, "Experimental observation of narrow surface plasmon resonances in gold nanoparticle arrays," Appl. Phys. Lett. **93**, 181108 (2008).
16. W. Huang, W. Qian, P. K. Jain, and M. A. El-Sayed, "The effect of plasmon field on the coherent lattice phonon oscillation in electron-beam fabricated gold nanoparticle pairs," Nano Lett. **7**, 3227–3234 (2007).
17. P. B. Johnson and R. W. Christy, "Optical constants of the noble metals," Phys. Rev. B **6**, 4370–4379 (1972).
18. A. Ghoshal and P. G. Kik, "Theory and simulation of surface plasmon excitation using resonant metal nanoparticle arrays," J. Appl. Phys. **103**, 113111 (2008).
19. N. Felidj, J. Aubard, G. Levi, J. R. Krenn, A. Hohenau, G. Schider, A. Leitner, and F. R. Aussenegg, "Optimized surface-enhanced Raman scattering on gold nanoparticle arrays," Appl. Phys. Lett. **82**, 3095–3097 (2003).
20. M. G. Banaee and K. B. Crozier, "Mixed dimer double-resonance substrates for surface-enhanced Raman spectroscopy," ACS Nano **5**, 307–314 (2011).
21. A. Ghoshal, I. Divliansky, and P. G. Kik, "Experimental observation of mode-selective anticrossing in surface-plasmon-coupled metal nanoparticle arrays," Appl. Phys. Lett. **94**, 171108 (2009).
22. Y. Sonnefraud, N. Verellen, H. Sobhani, G. A. E. Vandenbosch, V. V. Moshchalkov, P. Van Dorpe, P. Nordlander, and S. A. Maier, "Experimental realization of subradiant, superradiant, and Fano resonances in ring/disk plasmonic nanocavities," ACS Nano **4**, 1664–1670 (2010).
23. J. Gao, J. F. McMillan, M. C. Wu, J. Zheng, S. Assefa, and C. W. Wong, "Demonstration of an air-slot mode-gap confined photonic crystal slab nanocavity with ultrasmall mode volumes," Appl. Phys. Lett. **96**, 051123 (2010).
24. P. T. Kristensen, C. Van Vlack, and S. Hughes, "Generalized effective mode volume for leaky optical cavities," Opt. Lett. **37**, 1649–1651 (2012).
25. P. K. Jain, W. Huang, and M. A. El-Sayed, "On the universal scaling behavior of the distance decay of plasmon coupling in metal nanoparticle pairs: a plasmon ruler equation," Nano Lett. **7**, 2080–2088 (2007).
26. P. K. Jain, S. Eustis, and M. A. El-Sayed, "Plasmon coupling in nanorod assemblies: optical absorption, discrete dipole approximation simulation, and exciton-coupling model," J. Phys. Chem. B **110**, 18243–18253 (2006).
27. K. D. Osberg, N. Harris, T. Ozel, J. C. Ku, G. C. Schatz, and C. A. Mirkin, "Systematic study of antibonding modes in gold nanorod dimers and trimers," Nano Lett. **14**, 6949–6954 (2014).